

## Compact Modeling of SiC Schottky Barrier Diode (SBD) and Its Extension to Junction Barrier Schottky Diode (JBS)

Dondee Navarro<sup>1</sup>, Mitiko Miura-Mattausch<sup>1</sup>, Hans Jürgen Mattausch<sup>1</sup>, Mamoru Takusagawa<sup>2</sup>, Jun Kobayashi<sup>2</sup>, and Masafumi Hara<sup>2</sup>

<sup>1</sup> HiSIM Research Center, Hiroshima University, 1-3-1 Kagamiyama, Higashihiroshima, Hiroshima 739-8530, Japan

Phone: +81-82-424-7018 E-mail: dondee-navarro@hiroshima-u.ac.jp

<sup>2</sup> Toyota Motor Corporation, Nishihirose-cho, Toyota, Aichi 470-0309, Japan

### Abstract

We have developed a compact model applicable for both Schottky Barrier Diode (SBD) and Junction Barrier Schottky Diode (JBS) structures. The model considers the thermionic emission current in the metal/semiconductor junction together with the distributed resistance of the lightly doped drift region. Extension of the model to JBS is accomplished by considering the geometrical features induced by the  $p^+$  implant. Accurate reproduction of SiC JBS current-voltage measurements is achieved for different temperatures.

### 1. Introduction

SiC-based devices are presently being employed in high-power and high-temperature applications where conventional semiconductors cannot adequately function. Two types of SiC-based power diodes: Schottky Barrier Diode (SBD) and Junction Barrier Schottky Diode (JBS), shown in Fig. 1, are used as rectifiers in converters [1-4]. JBS structure is based on SBD with the addition of  $p^+$  implant to minimize the inherently large reverse tunneling current in SBD.  $p^+$  implant extends depletion to the  $n$ - drift region which inhibits tunneling. However,  $p^+$  region creates a distributed resistance in the adjacent  $n$ - region which modifies the SBD forward characteristics. Fig. 2 shows the simulated  $I$ - $V$  characteristics of SBD and JBS for different  $p^+$  implant widths  $W_p$ . The effective width at the anode side becomes  $W_{\text{cell}} - W_p$  for JBS. If the SBD current is calculated with varying widths of  $(W_{\text{cell}} - W_p)/W_{\text{cell}}$ , the resulting currents are less than that of the JBS. Such issue should be addressed to fully utilize SBD and its extended structure JBS. Our goal is to develop a unified compact model for both structures beneficial for power circuit simulation and device optimization.

### 2. 2D Device Simulation and Compact Modeling

2D device simulation reveals that in SBD, the electron current density  $J$  is uniform throughout the body but in JBS,  $J$  becomes concentrated in the  $n$ - region adjacent to the  $p^+$  implant as shown in Fig. 3(a). Fig. 3(b) shows a uniform  $J$  along A ( $y=L_{\text{cell}}$ ). Along B ( $y=0.25L_{\text{cell}}$ ),  $J$  starts to peak towards the  $n$ - region near the  $p^+$  implant. Along C ( $y=0.5L_p$ ),  $J$  is highest at the  $n$ - region. As the width opening  $W_{\text{cell}} - W_p$  decreases, the peak increases, whereas the current injection from the bottom decreases. This decrease in injection reveals the high resistant effect of the drift region. The electron current density from the drift region then becomes concentrated in the  $n$ - area adjacent to  $p^+$  and flows out to the anode as illustrated by the lines in Fig. 4. A relation

$$J_2 = J_0 \cdot \left[ 1 + W_p / (W_{\text{cell}} - W_p) \right] \quad (1)$$

can be derived when  $J_2 = J_0 + J_1$ , and  $J_0$  is equal to  $J_1$ . It is also observed that the effective width of the  $n$ - anode is less than  $W_{\text{cell}} - W_p$  because of the depletion in the  $p^+/n$ - junction. This means that  $W_p$  is modulated by the depletion width  $W_{\text{dep}}$ . The relation in Eq. 1 has the same feature as the peak current density along C for different  $W_p$  as shown in Fig. 5. This means that the current increase in the  $n$ - region can be described by the  $p^+$  geometry only.

The potential distribution along the length of the SBD and JBS diodes are shown in Fig. 6. For SBD, the potential is a straight line throughout the drift region. For JBS, the straight line abruptly rises at the  $p^+$  implant length  $L_p$ .

To obtain a unified modified considering the different phenomena observed, the developed equivalent circuit for the model is shown in Fig. 7. The diode is connected to two resistors  $R1$  and  $R2$ . Diode current is given by thermionic emission [5]. The currents through  $R1$  and  $R2$  are modeled as

$$I_{R1} = qN_d\mu \frac{AREA}{(L_{\text{cell}} - L_p)} \cdot V(N1, \text{cathode}) \quad (2)$$

$$I_{R2} = qN_d\mu \frac{AREA'}{L_p} \cdot \frac{1}{1 + W_p / (W_{\text{cell}} - W_p)} \cdot V(N2, N1) \quad (3)$$

where  $N_d$  is the impurity concentration of the drift region and  $\mu$  is the carrier mobility.  $V(N1, \text{cathode})$  and  $V(N2, N1)$  are the potentials across the diode,  $R1$  and  $R2$ , respectively. The modification of the area of  $R2$  due to the  $p^+$  implant is given by  $AREA' = AREA \cdot (W_{\text{cell}} - W_p) / W_{\text{cell}}$ .  $AREA$  refers to the cathode area. Depletion width  $W_{\text{dep}}$  from the  $p^+/n$ - junction is added to  $W_p$ . The geometric factor in Eq. 3 came from Eq. 1 to modulate the distributed resistance  $R2$ . As  $W_p$  increases,  $R2$  decreases which means higher current density flows in the  $n$ - region near the anode.

### 3. Verification with Device Simulation and Measurements

Fig. 8 shows the SBD current characteristics of the developed model in comparison with 2D device simulation results. By including the  $p^+$  geometry, the model is verified to fit JBS characteristics for different  $W_p$  as shown in Fig. 9. The potential across the diode body calculated by the model is depicted by the circles in Fig. 6.

Comparison with measurements for  $W_p = 0.4W_{\text{cell}}$  is shown in Fig. 10 for different temperatures where the temperature dependence is included in the phonon mobility and the Richardson constant. Measurements are accurately reproduced.

### 4. Conclusion

A unified compact model applicable for both SBD and JBS diode structures is developed based on thermionic emission and distributed resistance of the drift region of the diode. Good agreement with JBS  $I$ - $V$  measurements is verified. The model can be well-applied even for device optimization.

**References**

- [1] R. Simanjorang, et al., Applied Power Electronics Conf., 2010.
- [2] R. Singh, et al., IEEE Trans. Elec Devices, 2002.
- [3] F. Hirokazu, et al., Materials Science Forum 2011.
- [4] E. V. Brunt, et al., Int. Sym. on Power Semicon. Dev. and IC's, 2016.
- [5] S. M. Sze, Physics of Semiconductor Devices, 1981.

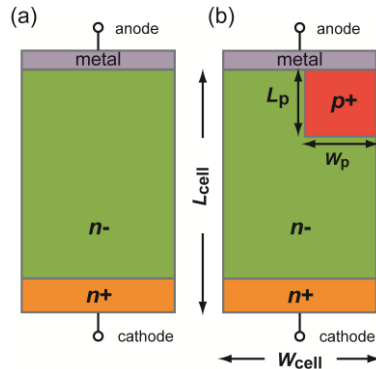


Fig. 1. (a) Schottky Barrier Diode (SBD) and (b) Junction Barrier Schottky Diode (JBS) structures.

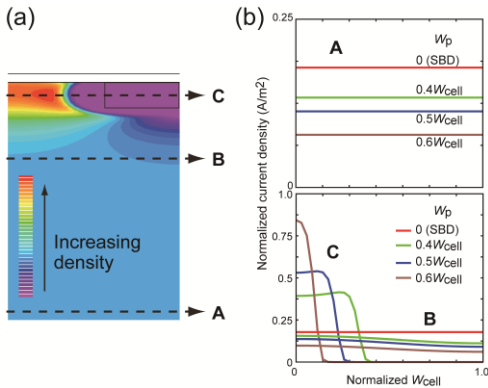


Fig. 3. (a) Electron current density in a JBS cross-section. JBS has a peak density at the  $n^-$  region adjacent to the  $p^+$  implant. (b) Current density at A:  $y=L_{cell}$ , B:  $y=0.25L_{cell}$ , and C:  $y=0.5L_p$ .

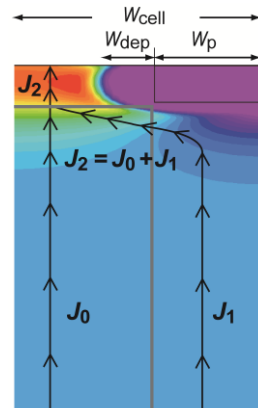


Fig. 4. Schematic illustration of electron current flow.

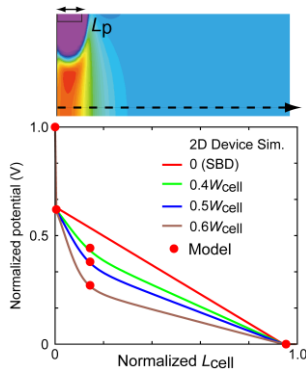


Fig. 6. Potential distribution along the  $n^-$  drift region of SBD and JBS. Potential calculated by the developed model is depicted by circles.

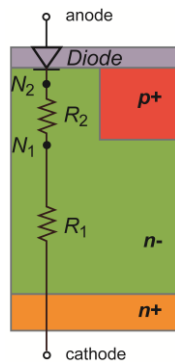


Fig. 7. Developed equivalent circuit. A diode is connected to two resistances to model the distributed resistance of the SBD and JBS diode structures.

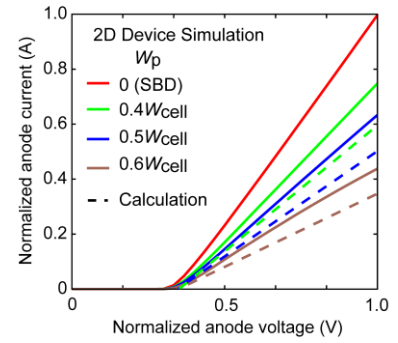


Fig. 2. SBD and JBS current characteristics by 2D device simulation. Dashed lines are SBD current calculated with  $(W_{cell}-W_p)/W_{cell}$ .

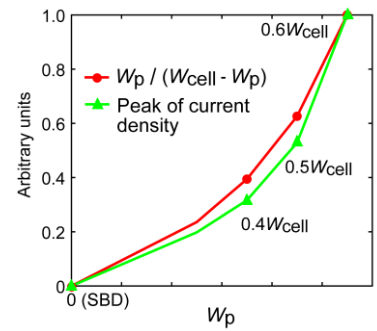


Fig. 5. The peak of current density along C in Fig. 3(b) has the same features as Eq. 1. Therefore, current density for JBS can be described by the geometrical features of the  $p^+$  implant.

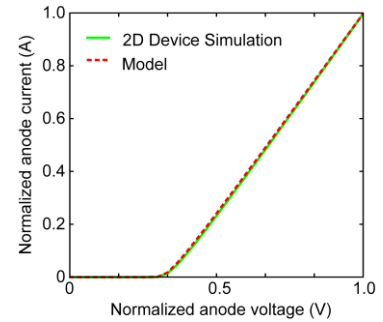


Fig. 8. SBD current calculated by the developed model compared to 2D device simulation results.

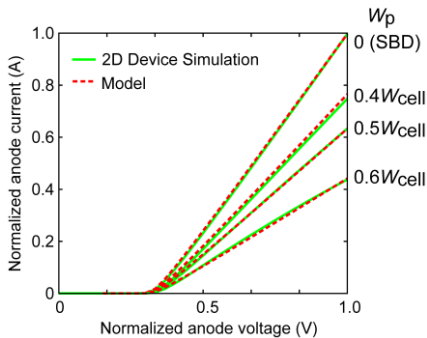


Fig. 9. JBS currents for different  $p^+$  implant widths calculated by the developed model compared to 2D device simulation results.

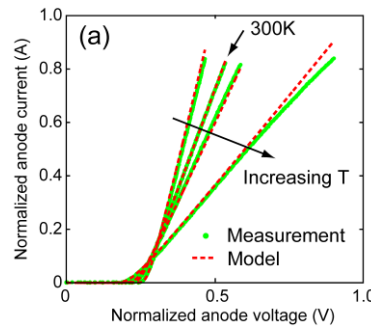


Fig. 10. (a) Linear and (b) log plots of SiC JBS  $I-V$  characteristics at different temperatures calculated by the developed model compared to measurements.